Short Communication

Effects of infill orientation and percentage on the magnetoactive properties of 3D printed magnetic elastomer structures

James M. Ennis [a],*, Hannah G. Thatcher [a], Thomas M. Calascione [a], Jimmy Lu [a], Nathan A. Fischer [a], Sarah J. Ziemann [a], Thomas Höft [b], Brittany B. Nelson-Cheeseman [a]

[a] *Department of Mechanical Engineering, University of St. Thomas, St. Paul, MN, USA, 55105*
[b] *Department of Mathematics, University of St. Thomas, St. Paul, MN, USA, 55105*

A B S T R A C T

This work investigates how the internal meso structure of fused filament fabrication parts influence the magnetoactive properties of printed magnetic elastomer structures. Elastomers were made by adding 40 wt% magnetite (Fe_3O_4) to a thermoplastic polyurethane (TPU) matrix. Magnetoactive testing was used to investigate how varying the infill structure affected the mechanical response of the structures within an applied magnetic field. Different infill percentages (40%, 60%, and 100%) and infill orientations (0, 45, and 90 degrees) were tested to account for different mechanical stiffnesses and internal geometries. Each sample was magnetoactively tested with three transverse magnetic field orientations (front, back and top). The samples were placed between two electromagnets, and the angle of deflection was recorded as a function of applied field. The maximum angles of deflection for the testing setup were reached when using lower infill percentages and having infill oriented parallel to the long axis of the sample and transverse to the magnetic field. Transverse fields applied parallel to the print plane (front/back sample orientations) demonstrated the most magnetoaction due to easier alignment of the long side of the sample with the field. This coupled with the 0-degree infill orientation having less crosslinking constraining the bending stiffness led to greater deflection. The magnetic anisotropy of the infill structure likely also contributed to the large response from certain samples. It was concluded that for this fixed base material, it is more important to 3D print structures with lower stiffnesses than more net magnetic particulate (more infill) to achieve the most magnetoaction.

1. Introduction

Magnetic elastomers are flexible smart materials that can be manipulated by magnetic fields to achieve reversible mechanical deformation [1]. These highly configurable materials deform with applied magnetic fields due to the inclusion of magnetic particulate embedded within the elastomer matrix. These materials can be used for many different applications from magnetic actuators to soft robotics [2–6]. In soft robotics, these elastomers can be used to create artificial muscles and other bio-actuators which give the robot both power and control [7]. These elastomers can also be used in the following: remotely moveable micro-grippers for gripping fragile objects, valves for controlling fluid flow using remote magnetic field actuation, and soft skins that can either sense touch and local deformations or reversibly deform for applications such as rewritable braille displays [8]. Various properties are exhibited within these materials depending on the type of magnetic particulate and physical structure.

Using fused filament fabrication (FFF), it was recently found that magnetic polymer composite structures could be created that take advantage of unique internal geometries to tune certain properties. [9,10]. FFF is a 3D-printing process where material is extruded in 1D lines (infill) to build 2D planes layer-by-layer, resulting in a 3D structure. Structures with different levels of anisotropy and complicated interior geometries (infill) can be created enabling control of both the magnetic and mechanical properties of the part. Typically, more rigid materials are used for FFF, but flexible materials including elastomers have become more common.

Although the effect of the highly customizable infill configurations on the magnetoactive properties of magnetic elastomers has not yet been reported, previous research has shown that differing FFF infill settings on nonmagnetic polymeric structures including elastomers can change their mechanical properties [11–13]. The parts tend to be stiffer the greater the infill percentage and the more aligned the infill with the direction of loading [14,15]. Previous research in magnetic elastomers has shown that parts magnetize most quickly when the infill direction is parallel to the applied magnetic field, and this effect is most striking for lower infill percentages [9,10,16]. With lower infill percentages, however, the overall magnetic particulate amount will be decreased since the amount of material within the sample will be decreased. This presents a conundrum, since lower infill produces less stiffness mechanically, while magnetically lower infill produces less magnetic moment. Since these two parameters compete with one another and the magnetoactive performance of magnetic elastomers is a convolution of both their mechanical and magnetic responses, one would expect that optimization the magnetoactive response of 3D printed magnetic elastomers would require tuning of infill orientation and infill percentage.

In this work, the effects of the infill percentage and infill orientation on the magnetoactive response of FFF printed magnetic elastomers were investigated and categorized. Different infill percentages (40%, 60%, and 100%) and different infill orientations (0, 45, and 90°) were tested to account for different internal geometries. The material used was a magnetite particulate mixed into a thermoplastic polyurethane polymer base matrix. The transverse deflection of printed rectangular beams was optically tracked in the presence of a transverse magnetic field. This simplified experimental setup and sample set enabled the underlying contributing factors to be clearly isolated for the displayed behavior of the samples. Samples with lower infill percentages and more perpendicular infill orientation relative to the applied magnetic field exhibited the greatest magnetoactive response.

2. Methods

The samples will be discussed in terms of their micro, macro, and meso (infill) structure.

2.1. Filament properties

This project explored the magnetoactive properties of 3D-printed magnetic elastomers made with 40 wt% magnetite, Fe_3O_4, with a thermoplastic polyurethane (TPU) matrix. The magnetite was blended with the TPU prior to printing to create a stock composite filament as described in References 17 and 18. Spherical magnetite particulate 2-4 microns in size was used to ensure the least amount of clogging occurred in the printer [18,19]. Micron size particulate was used as opposed to nano size particulate due to the availability of the particulate in the large quantities necessary for these milli/macro-scale applications. The base matrix of the composite was TPU, a filament material commercially made by NinjaTek [20]. Due to its moisture absorbent nature, the magnetite TPU filament had to be dehydrated for a few hours before use to prevent detrimental air bubbles while printing.

2.2. Sample design

The macro structures printed for all infill settings were rectangular beams measuring 60 mm by 5 mm by 5 mm. This macro structure as well as the meso structure of samples at 40% infill can be seen in Fig. 1.
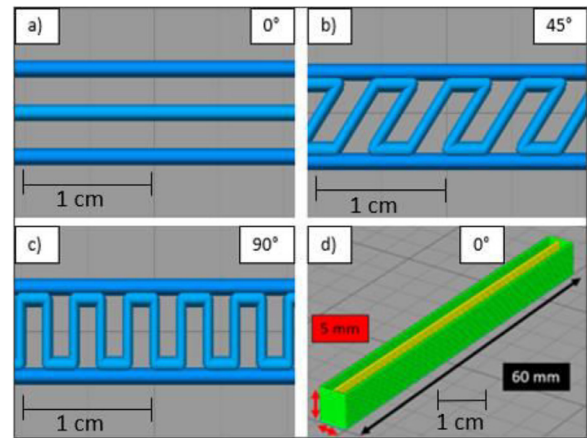

Fig. 1. Schematic sample infill orientations for (a) 0-degree, (b) 45-degree, and (c) 90-degree (relative to the horizontal or longitudinal axis of the sample) at 40% infill, (d) Isometric view of a sample with 0-degree 40% infill showing interior structure (yellow) and perimeter structure (green) with dimensions of $60 \times 5 \times 5$ mm^3 (For interpretation of the references to color in this figure caption, the reader is referred to the web version of this article.)

An isometric view of a beam at 0-degrees, 40% infill (yellow) can be seen in Fig. 1d. All the beams were printed without a top or bottom shell layer such that the meso structure was exposed as can be seen in Fig. 1d. The meso structure of the printed samples included three different infill orientations (0°, 45° and 90°) as shown in Fig. 1(a-c). The infill orientation controls the angle of the infill with respect to the longitudinal axis of the sample. Each of these samples were printed with infill percentages of 40%, 60% and 100% respectively, to ensure structures with a range of mechanical stiffnesses and overall magnetic particulate content were tested. The infill percentage controls the amount of material used in creating the interior structure of the sample. Despite changing the infill percentage and orientation (meso structure), the weight percent of the particulate within the TPU matrix (microstructure) remained the same throughout all the printed samples. A comprehensive display of all the infill percentage and orientation combinations can be seen in Fig. 2 along with the top view of a 0-degree, 60% infill sample. The ability of FFF to create anisotropy can be seen in Fig. 1(a,d),
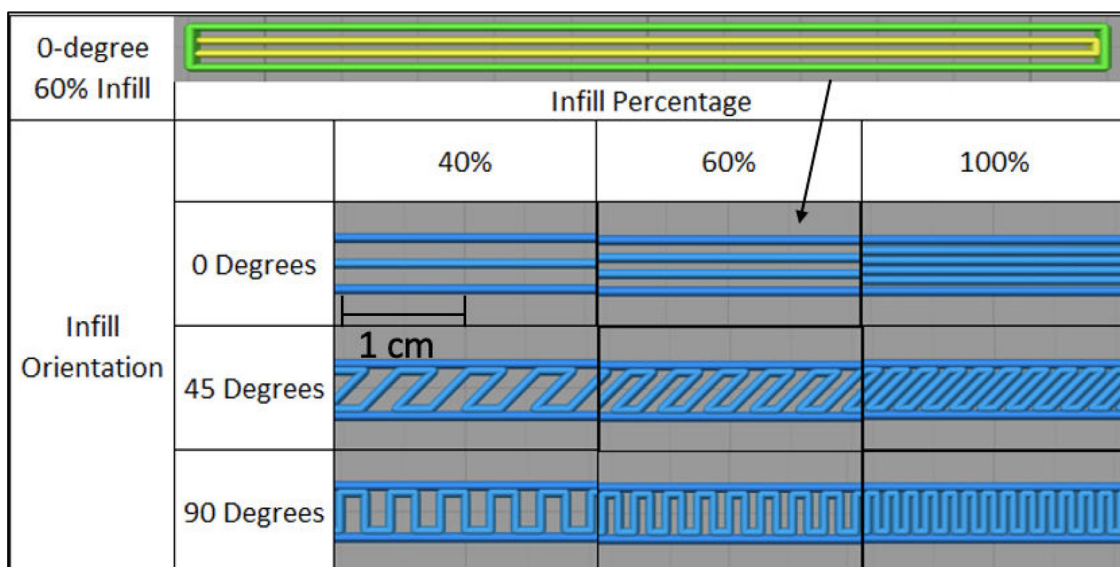

Fig. 2. All sample types tested showing infill percentages and orientations, as well as full length top view of 0-degree 60% infill sample for reference, where the green and yellow simply represent the perimeter and interior infill, respectively, but do not represent any change in material used. (For interpretation of the references to color in this figure caption, the reader is referred to the web version of this article.)
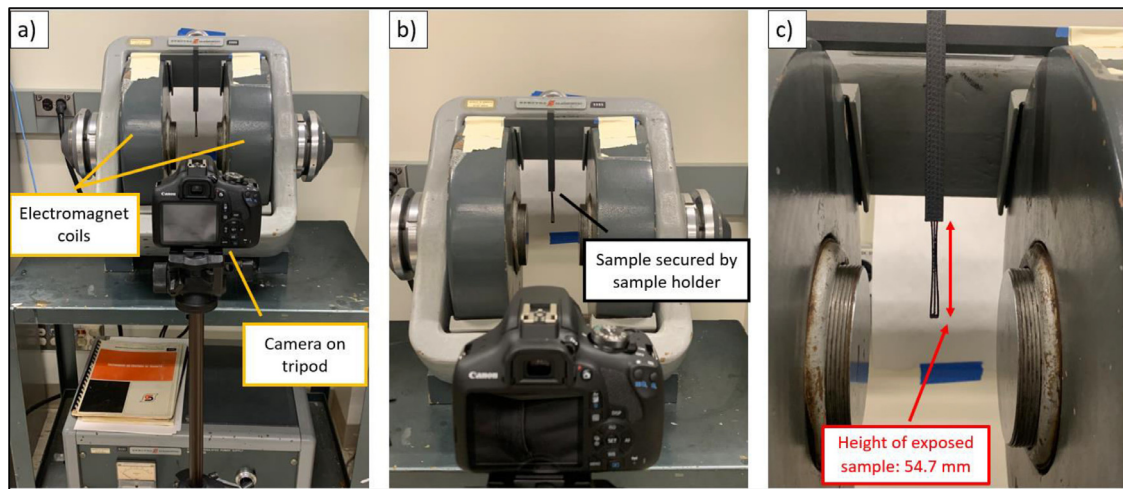
Fig. 3. Magnetoactive testing setup. (a,b) Camera and tripod aimed at sample between electromagnet, and (c) electromagnet and sample including exposed sample height of 54.7 mm.

and Fig. 2 with the 0-degree infill orientation. The infill is parallel to the longitudinal axis and thus oriented in that direction as opposed to the transverse direction which means the properties, both magnetic and mechanical, will differ in the long axis direction versus the transverse direction [9]. Fig. 2 shows how the infill percentage affects the negative space within the perimeters of the samples. As the infill percentage increases, the negative space decreases meaning there is more composite material inside the perimeter of the sample.

2.3. Filament extrusion and sample printing

The composite material used was not an ink as is sometimes used in FFF printing, but rather a thermoplastic polyurethane filament that had already been impregnated with particulate using an extrusion-based method [17,18]. The composite material was made by solvent casting, which involved dissolving TPU in a dimethylformamide (DMF) bath and then adding in the magnetite particulate. The DMF was then evaporated out of the TPU particulate mix, and the composite was extruded through an Ex 2 Filabot extruder with a 1.75 mm nozzle [17,18]. The filament was then used for printing on a Lulzbot Mini 2 3D Printer where it was heated and extruded in 1D lines (infill) to build 2D planes layer-by-layer, resulting in a 3D structure. No magnetic annealing or post-processing such as curing was used in this experimental setup.

The samples used were built using the computer-aided design software SolidWorks. These structures were converted to stereolithography files (STLs) and put into either of the two slicer softwares used, Simplify3D or Cura. Simplify3D was used due to its familiarity and ease of use since it had been used in previous research [14]. Cura was used for specific samples because it had more extensive and detailed settings which helped with samples that were difficult to print. Triplicates were made of each sample to ensure the most accurate data was gathered. The samples were printed at 235-240 °C to ensure that the filament had low viscosity and would flow smoothly [21]. The extrusion width, which is the base width of the infill and perimeter wall thickness, was set to 0.8 mm. The infill wall thickness could be tweaked as a percentage of the extrusion width and was typically left at 100-120% since the printer tended to under extrude due to the particulate clogging the nozzle. When the particulate would dislodge, however, there would be a sudden rush of material causing inconsistencies. These inconsistencies had to be addressed by changing the extrusion width values for certain prints by small margins depending on the consistency of that stretch of filament. The print speed also had an impact on the filament traveling smoothly through the nozzle. The slower the speed the more reliable the flow of filament through the nozzle, yet also the more likely it was to over ex-

trude at a certain point. It was thus held at 10 mm/s for all prints. The layer height of the prints was held constant at 0.3 mm [22]. The other less influential print settings were optimized and for the most part kept constant to achieve the best quality prints. A 0.8 mm nickel-plated brass nozzle was used to avoid clogging in the printing process and to avoid erosion due to the abrasive particulate which could cause a larger than desired nozzle diameter.

Due to the nature of the flexible filament, there were difficulties with kinking where the filament would take the path of least resistance and exit the side of the filament guide just before the hot end. This was due to built-up pressure from the hot end caused by clogging. To remedy this issue and to ensure the least number of clogs, the print head was cleaned regularly.

2.4. Scanning electron microscopy

Samples were examined using a scanning electron microscope (SEM) to investigate the surface roughness of the printed samples. This investigation was done to try to correlate the meso structure of the samples with their associated magnetoactive properties. The SEM was set to detect secondary electrons since this mode provided topographical information about the sample.

2.5. Magnetoactive testing

The procedural setup for the magnetoactive testing can be seen in Fig. 3(a-c). The camera was setup on a tripod to avoid any movement while taking the pictures that were referenced to one another. The Gauss meter was used to calculate the exact field output from the electromagnet. The sample holder was used to secure the sample in place between the magnets to restrict rotation of the sample and ensure deflection was the only source of movement. The height of the exposed part of the sample to the field was 54.7 mm for each sample.

Magnetoactive testing was done on all infill percentage and orientation combinations seen in Fig. 2 to characterize how the magnetic elastomer material mechanically responded to an applied magnetic field when printed with different infill percentages and orientations. We note that the ratio of magnetic particulate to TPU was held constant throughout all infill percentages and orientations as the same base composite filament was used for all sample printing. However, it is important to highlight that as the infill percentage decreased, the overall net magnetic particulate content within the sample decreased, as there was less composite material contained within the sample beam volume, resulting in a smaller magnetic moment.
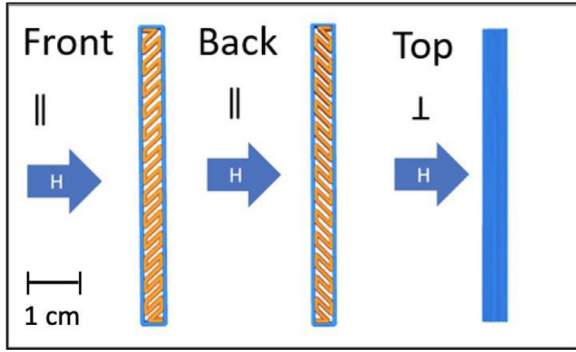
Fig. 4. Three different orientations of the same 45-degree infill sample in relation to the applied magnetic field (H) with orange indicating the infill of the printed sample. (For interpretation of the references to color in this figure caption, the reader is referred to the web version of this article.)

Fig. 5. Overlayed image of 0-degree 40% infill sample at 0 T with image of sample at 0.28 T.

The magnetoactive testing was done at the University of Minnesota where the samples were placed between an electromagnet emitting up to a 0.4 T field. The electromagnet was a 4-inch Adjustable Gap Laboratory Electromagnet made by Spectromagnet Industries with model number 1019. The angle of deflection was recorded as a function of applied field by overlaying pictures taken at each field strength with the sample at 0 T before saturation as the reference. The sample was then saturated by turning the field strength to 0.4 T since that was the max field strength that the electromagnet could provide with the largest width between the two electromagnets. The first angle measurement was then taken at 0 T after saturation. The sample was not vertical anymore and thus displayed an angle of deflection at 0 T after saturation due to the remnant magnetization. The field strength was controlled by changing the amperage of the electromagnet. This amperage was increased in increments of 5 amps from 0 to 30 amps, which produced an increasing magnetic field in increments of about 0.07 T. To achieve accurate magnetic field measurements, the field strength was measured with a gauss meter that was placed at the location of the sample within the field.

Fig. 4 shows the three different sample orientations (front, back, top) with respect to the applied field using a 45-degree infill orientation. These three different magnetoactive testing orientations were used to account for any magnetoactive effects that occurred due to the print layering or infill orientation. This simplicity of the setup allowed the for the clear characterization of the magneoactive behavior of the samples.

2.6. MATLAB image analysis

The images were analyzed using a MATLAB program. To determine the angle of deflection, a series of image processing steps were performed on the reference image of the structure at 0 T and on an image of the deflected structure. An example of the reference image at 0 T with an overlayed image at 0.28 T can be seen in Fig. 5.

In both images, the program identified the pixel locations of the upper-left and lower-left corners of the structure and calculated the slopes of the line from upper-left to lower-left corners, m_ref for the reference and m_def for the deflected. From these slopes, the angle in radians between the lines was found using Eq. (1).

$$\theta = \tan^{-1}((m_{ref} - m_{def})/(1 + m_{ref} * m_{def})) \tag{1}$$

3. Results/discussion

3.1. SEM images of 45 degree printed sample

The samples were inspected using a SEM to examine the surface texture and consistency in the 3D printer extrusion. The images of the top and bottom of two samples can be seen in Fig. 6(a) and 6(b) respectively.
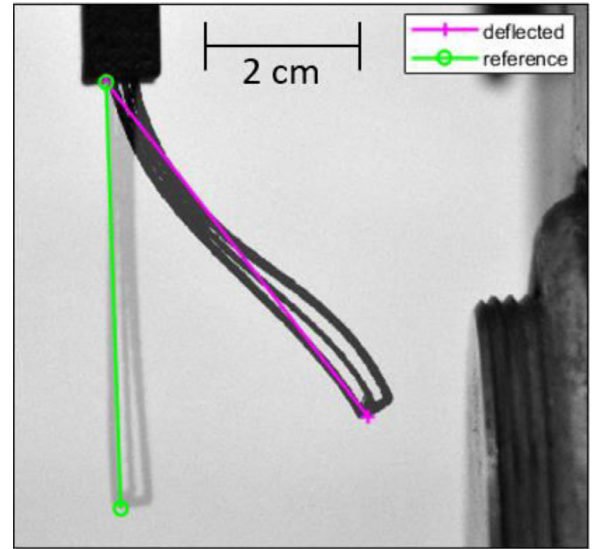
These images indicate that the surfaces of the top and bottom layers have different levels of roughness. The bottom of the printed part is pressed against the print plate making it smooth, while the top is susceptible to stringing from the nozzle pulling material as it moves instead of laying it all down cleanly. The infill lines for both sides are not as pristine as indicated by the slicer software Simplify3D. These features were found across the different sample types printed, and thus do not account for the property differences seen as a function of infill percentage and direction. While large changes to the *micro*structure are not anticipated from merely the various *meso*-scopic infill parameters studied here, we do note that changes to the microstructure from additional variables (such as magnetic annealing, particulate volume percentage, particulate shape, particulate size, particulate material type, etc.) are ripe for exploration to further tune the magnetoactive properties in these structures.

3.2. Magnetoactive testing

The samples were tested to determine the effect of infill percentage and orientation on the magnetoactive properties of the sample. Noticeable deflection in response to the applied magnetic field was seen in the 0-degree 40% and 60% infill samples in the front and back orientations. All other samples demonstrated no noticeable response to the applied field. This provides clear evidence for the importance of infill structure on achieving sizeable magnetoactive properties. The quantitative results can be seen in Fig. 7, and the qualitative results containing the pictures of samples at each field can be seen in Fig. 8. The error bars in Fig. 7 were calculated using the absolute uncertainty from each set of angles for each infill percentage, infill orientation, and sample orientation. The increase in error bar length is correlated to the increase in slope of the graph.

As the angle of deflection increased more drastically from one field strength to another, the error within the triplicates got larger. This made sense since the more movement there was within a given sample, the higher the likelihood of variability within the different sample angles. Despite the slightly overlapping error bars, in general, the average angle of deflection increased with increasing applied field.

Some of the samples reached the maximum possible angle afforded by the testing setup before the maximum field strength was reached resulting in the plateau in angle measurements at the largest field strengths. Note that there are two points recorded in Fig. 7 at 0 T for each sample type: one at 0° and one greater than 0°. The non-zero
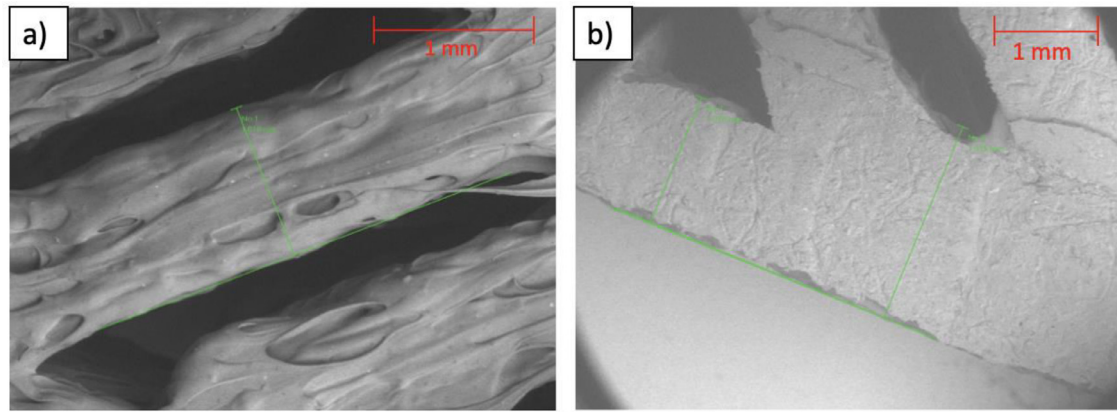
Fig. 6. (a) The top side of a 45-degree printed structure, (b) The bottom side of a 45-degree 3D printed structure.
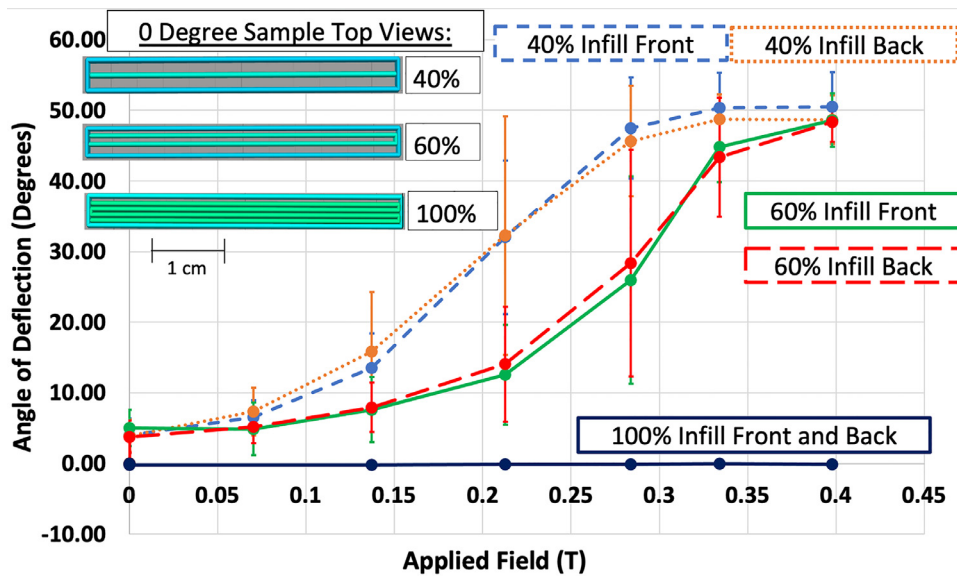

Fig. 7. 0°, 40%, 60%, and 100% infill samples all front and certain back orientations showing trends in angle of deflection for increasing magnetic fields.

deflection angle at 0° was due to the remnant magnetization after saturating the sample. The images of the samples at each applied field strength, including at 0 T after the initial saturation, can be seen in Fig. 8. The reason the top orientation is not seen in Fig. 8 is because it did not deflect enough to be measured, as seen in Fig. 8.

3.2.1. Infill percentage effect

Lower infill percentage resulted in greater magnetoaction, as seen from the behavior of the samples in Fig. 7. For a given applied magnetic field, the 40% infill had the greatest magnetoaction, the 60% infill had slightly less, and the 100% infill had no noticeable magnetoaction for the fields measured. When considering the overlapping error bars, it is well known that for both additively manufactured and composite materials, there is inherent structural variability within nominally identical structures that can contribute to property variability. The Rule of Mixtures in composite materials specifically highlights that there are upper and lower bounds to the anticipated properties of a given composite material composition due to the uncertainties of the exact geometrical dispersion of the dispersed phase. [23] This applies to the anticipated mechanical stiffness values for a given composite composition, which directly affects the magnetoactive response. Despite this anticipated deviation due to these factors, we note that on average there is still a noticeable difference between the 40% infill and 60% infill samples. Additionally, there is clearly a difference between the lower infill percentages and the 100% infill sample. Both aspects support the conclusion that lower infill percentage leads to larger magnetoaction in these structures, despite the lower amount of magnetic material present.

To understand this effect on magnetoaction, it is helpful to consider both the mechanical and magnetic implications of infill percentage. Mechanically, lower infill percentage means less internal material, which typically translates to lower stiffness, maximizing magnetoaction. Moreover, note that the 100% infill structures additionally have a maximum amount of internal connection between adjacent infill lines; this would further increase the stiffness of those samples and inhibit their magnetoaction. This result shows the direct correlation between infill percentage and stiffness, that as infill percentage increases so does the stiffness of the sample, inhibiting deflection. However, magnetically, lower infill percentage means less net magnetic particulate, minimizing magnetoaction. With less net magnetic particulate in the sample due to a less dense interior, one might expect that the lower infill percentage samples would be less magnetic and thus have a lower response to the applied field than the samples with more net magnetic particulate [22,24]. However, all the 100% infill samples at each infill orientation resulted in no measured magnetoactive deflection thus indicating that smaller stiffness does matter more than a larger net amount of magnetic particulate. The infill percentage trend observed here indicates that printing samples with lower mechanical stiffness as opposed to greater net magnetic particulate leads to the greatest magnetoaction.

3.2.2. Infill angle/orientation effect

In this study, only the 0-degree samples exhibited magnetoaction, while the 45 and 90-degree samples remained motionless. Given the conclusions discussed above about the importance of low stiffness, this behavior was reasonable. These samples required the least material for
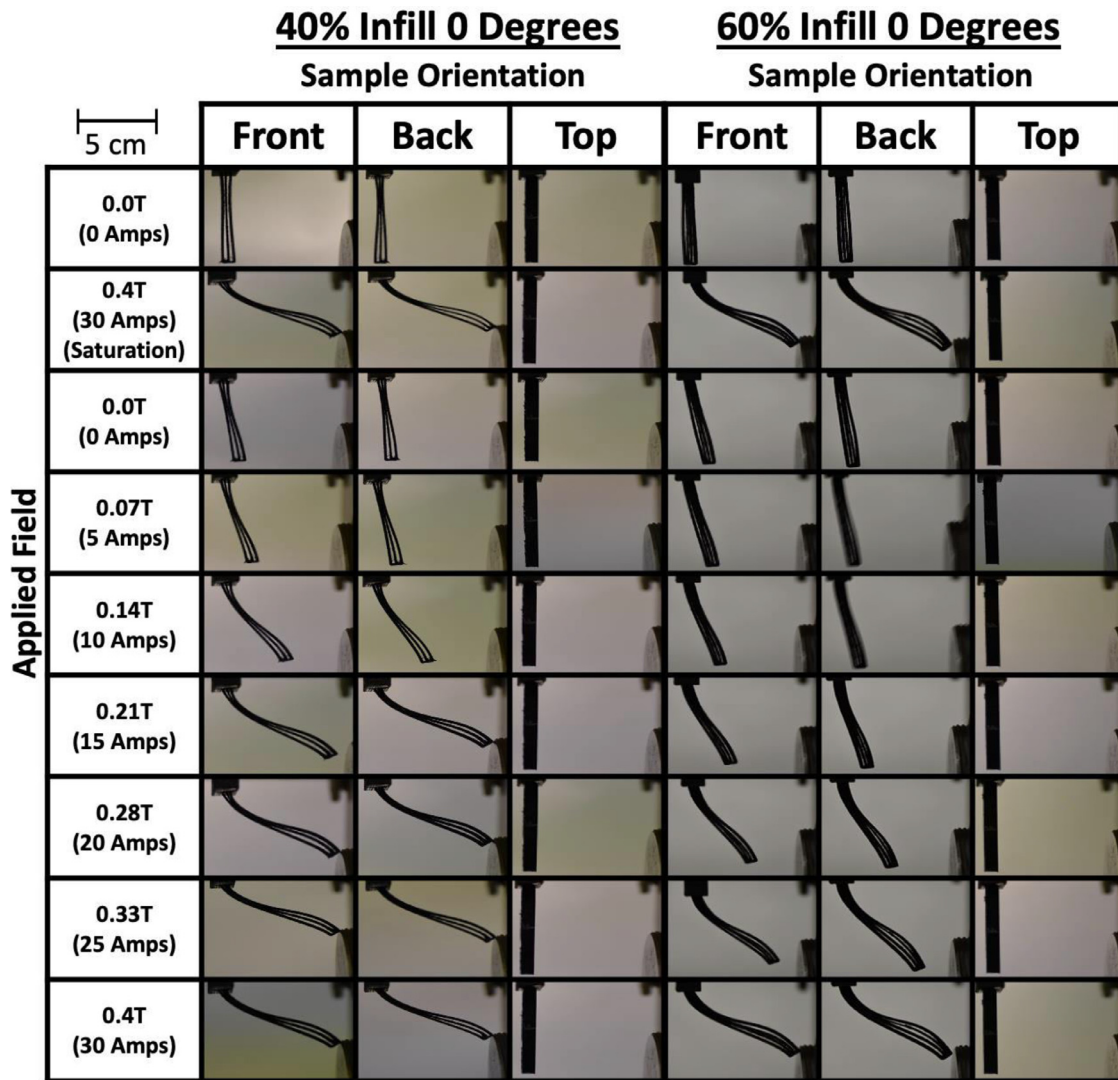
Fig. 8. Images of one of the 0-degree 40% and 60% infill triplicates in all tested orientations, showing measurable deflection for all field strengths including saturation.

creation and lacked the infill cross-linking patterns central to the 45 and 90-degree samples that provided greater stiffness. These cross-linking patterns or lack thereof connecting each of the long edges of the structures can be seen in Fig. 1(a-d) for samples at 40% infill. One may note that a small amount of infill is oriented along the long axis of the sample for the 45- and 90-degree infill orientations. To investigate the possible effects of this, the percentage of transverse vs parallel infill was estimated for both the 45- and 90-degree samples. Using trigonometry, the lengths of both the infill lines oriented along the longitudinal side as well as the lengths of the infill lines crossing the sample could be found. Using the ratio between these two lengths as well as the number of crossing lines and non-crossing lines, the percentage of infill oriented in the direction of the specified angle for the 45 and 90-degree samples was estimated. At 40% infill, about 60% of the interior infill was oriented at the 45-degree angle. At 60% infill, about 70% of the interior infill was oriented at the 45-degree angle. At 100% infill, about 90% of the interior infill was oriented in the 45-degree angle. The 90-degree angle percentages were estimated to be the same due to the increasing number of occurrences of transverse infill despite the lengths of the transverse infill being shorter. At lower infill percentages this would mean that there would be more infill aligned along the longitudinal axis which would maximize the anisotropic differences. These samples, however, did not

appear to deflect within the field demonstrating the lack of influence that this factor had on the magnetoaction of these samples. While these structural differences did not seem to play a role in this study, as none of these samples showed magnetoaction, we highlight this variable as important in future work.

Another possible reason for this behavior from the 0-degree samples was the anisotropic structure [9,25]. Anisotropy is when the properties of a structure are dissimilar in different directions within the sample. It arises from structural differences on either a macro-scale, meso-scale, micro-scale, or a combination of these. Due to the ease of manipulating infill settings using FFF, finetuning the anisotropic properties of a structure is quite simple and powerful especially for applications like soft robotics. Here, the relative anisotropy of the various samples tested was determined by combining the relative anisotropies of the macroscopic shape with the mesoscopic infill orientation. Due to the anisotropic long axis of the samples, the 0-degree infill along this long axis reinforced this anisotropy, which would result in more anisotropic mechanical and magnetic properties [10]. Meanwhile, the 45 and 90-degree samples directed some or all their infill along the short axis of the sample, opposing or counteracting the effects of the long axis of the sample, creating a more isotropic structure overall, leading to more isotropic mechanical and magnetic properties [9,10]. Thus, for the 0-degree samples when

the field came through the front of the suspended sample beam, the sample tried to align the most particulate possible with the field meaning that the sample would deflect quite far to the side to align its infill lines as parallel as possible with the field. This occurred because magnetic fields move most easily through magnetic material as opposed to air gaps. The field, therefore, moved the sample to be parallel with it such that it could take the path of least resistance. This phenomenon can be seen clearly in Figs. 5 and 8. Other infill orientations did not have this same infill alignment and thus did not have as much magnetic anisotropy [26].

3.2.3. Sample orientation effect

The three different orientations of the samples relative to the field, which can be seen in Fig. 4, also influenced the observed deflection. We note that this is intimately related to the print orientation and layering inherent to FFF, which is well known to create anisotropic properties parallel and perpendicular to the plane. The front and back orientations demonstrated the most magnetoactive deflection due to being the least stiff and resistive to deflection. These two orientations were very similar since the field was simply going through the opposite side of the sample when switched from the front to the back orientation. This led to comparable results from both orientations at a specific infill percentage as can be seen in Fig. 8. The top orientation exhibited no measured magnetoactive deflection at all infill percentages, which indicated greater stiffness. This behavior was reasonable, because the moment of inertia was smaller for the front and back orientations than the top. The moment of inertia for the front and back orientations depended on the width of each print line, approximately 0.8 mm, while the moment of inertia for the top orientation depended on the sample width, 5 mm. The small force from the applied magnetic field was thus not able to deflect the samples in the top orientation. Additionally, the discontinuity of magnetic material (air gaps) in the path of the magnetic field direction for the 40% and 60% 0-degree samples oriented in the front and back orientations gave those samples greater motivation to align with the magnetic field. This discontinuity of magnetic material along the applied field direction was not present for the top orientation since the flux lines could pass through the printed walls of the sample. This further minimized the need for the sample to deflect in the top orientation, suppressing magnetoaction. The bottom orientation was not measured due to the assumption it would display the same lack of results as the top since it would effectively be reversing the field direction in the top orientation.

4. Conclusion

In conclusion, this research helped identify how the magnetoactive properties of 3D-printed magnetic elastomer samples were affected by changing the infill settings of the printed structures. This work provided foundational knowledge on a new processing approach to magnetic elastomers (FFF) and a new design paradigm for approaching classic FFF-structures from two conflicting property realms (mechanical vs. magnetic). In particular, this research helped explore the dilemma of maintaining flexibility within the 3D-printed structure while also having enough overall magnetic particulate to preserve magnetoaction due to the large impact of stiffness. The most magnetoactive samples indicated the importance of having lower structural stiffness rather than more net magnetic particulate in achieving a noticeable response to a magnetic field. The importance of anisotropy both magnetically and mechanically was clear due to the striking differences in responses by the 0-degree samples compared to the 45 and 90-degree samples at low infill percentages, as well as those seen from different sample orientations of the same sample. According to this data, meticulously designed 3D printed magnetite-TPU structures are well suited for creating a device easily stimulated by a magnetic field, unlocking possibilities for the creation of artificial muscles, magnetic actuators, and micro-grippers in different fields [2–8].

Declaration of Competing Interest

The authors declare that they have no known competing financial interests or personal relationships that could have appeared to influence the work reported in this paper.

Data availability

Data will be made available on request.

Acknowledgments

References

[1] M. Lokander, B. Stenberg, Performance of isotropic magnetorheological rubber materials, Polym. Test. 22 (3) (2003) 245–251, doi:10.1016/s0142-9418(02)00043-0.

[2] B.A. Evans, B.L. Fiser, W.J. Prins, D.J. Rapp, A.R. Shields, D.R. Glass, R. Superfine, A highly tunable silicone-based magnetic elastomer with nanoscale homogeneity, J. Magn. Magn. Mater. 324 (4) (2012) 501–507, doi:10.1016/j.jmmm.2011.08.045.

[3] G. Filipcsei, I. Csetneki, A. Szilágyi, M. Zrínyi, Magnetic field-responsive smart polymer composites, Oligomers # Poly. Comp. # Mol. Imprint. (2007) 137–189, doi:10.1007/12_2006_104.

[4] Y. Kim, H. Yuk, R. Zhao, S.A. Chester, X. Zhao, Printing ferromagnetic domains for untethered fast-transforming soft materials, Nature 558 (7709) (2018) 274–279, doi:10.1038/s41586-018-0185-0.

[5] M. Wehner, R.L. Truby, D.J. Fitzgerald, B. Mosadegh, G.M. Whitesides, J.A. Lewis, R.J. Wood, An integrated design and fabrication strategy for entirely soft, autonomous robots, Nature 536 (7617) (2016) 451–455, doi:10.1038/nature19100.

[6] J. Kim, S.E. Chung, S.-.E. Choi, H. Lee, J. Kim, S. Kwon, Programming magnetic anisotropy in Polymeric microactuators, Nat. Mater. 10 (10) (2011) 747–752, doi:10.1038/nmat3090.

[7] R. Zhao, Y. Kim, S.A. Chester, P. Sharma, X. Zhao, Mechanics of hard-magnetic soft materials, J. Mech. Phys. Solids 124 (2019) 244–263, doi:10.1016/j.jmps.2018.10.008.

[8] N. Bira, P. Dhagat, J.R. Davidson, A review of magnetic elastomers and their role in Soft Robotics, Front. Robot. AI 7 (2020), doi:10.3389/frobt.2020.588391.

[9] T.M. Calascione, N.A. Fischer, T.J. Lee, H.G. Thatcher, B.B. Nelson-Cheeseman, Controlling magnetic properties of 3D-printed magnetic elastomer structures via fused deposition modeling, AIP Adv. 11 (2) (2021) 025223, doi:10.1063/9.0000220.

[10] M.V. Patton, P. Ryan, T. Calascione, N. Fischer, A. Morgenstern, N. Stenger, BB. Nelson-Cheeseman, Manipulating magnetic anisotropy in fused filament fabricated parts via macroscopic shape, mesoscopic infill orientation, and infill percentage, Addit. Manuf. 27 (2019) 482–488, doi:10.1016/j.addma.2019.03.026.

[11] M. León-Calero, S.C. Reyburn Valés, Á. Marcos-Fernández, J. Rodríguez-Hernandez, 3D printing of thermoplastic elastomers: Role of the chemical composition and printing parameters in the production of parts with controlled energy absorption and damping capacity, Polymers 13 (20) (2021) 3551, doi:10.3390/polym13203551.

[12] P. Płatek, K. Rajkowski, K. Cieplak, M. Sarzyński, J. Małachowski, R. Woźniak, J. Janiszewski, Deformation process of 3D printed structures made from flexible material with different values of relative density, Polymers 12 (9) (2020) 2120, doi:10.3390/polym12092120.

[13] T.D. Harpool, [dissertation], 2016, pp. 1–82.

[14] S.E. Nace, J. Tiernan, D. Holland, A. Ni Annaidh, A comparative analysis of the compression characteristics of a thermoplastic polyurethane 3D printed in four infill patterns for comfort applications, Rapid Prototyp. J. 27 (11) (2021) 24–36, doi:10.1108/rpj-07-2020-0155.

[15] C.-H. Liu, Y. Chen, S.-Y. Yang, Quantification of hyperelastic material parameters for a 3D-printed thermoplastic elastomer with different infill percentages, Mater. Today Commun. 26 (2020) 101895, doi:10.1016/j.mtcomm.2020.101895.

[16] A.K. Bastola, M. Hossain, A review on Magneto-mechanical characterizations of magnetorheological elastomers, Compos B Eng 200 (2020) 108348, doi:10.1016/j.compositesb.2020.108348.

[17] T.J. Lee, A.H. Morgenstern, T.H. Höft, B.B. Nelson-Cheeseman, Dispersion of particulate in solvent cast magnetic thermoplastic polyurethane elastomer composites, AIMS Mater. Sci. 6 (3) (2019) 354–362, doi:10.3934/matersci.2019.3.354.

[18] A.H. Morgenstern, T.M. Calascione, N.A. Fischer, T.J. Lee, J.E. Wentz, BB. Nelson-Cheeseman, Thermoplastic magnetic elastomer for fused filament fabrication, AIMS Mater. Sci. 6 (3) (2019) 363–376, doi:10.3934/matersci.2019.3.363.

[19] W.H. Li, X.Z. Zhang, A study of the magnetorheological effect of bimodal particle based magnetorheological elastomers, Smart Mater. Struct. 19 (3) (2010) 035002, doi:10.1088/0964-1726/19/3/035002.

[20] Ninjatek Ninjaflex water semi-transparent TPU filament - 1.75mm (0.5kg). MatterHackers. [accessed 2022 Jan 11]. https://www.matterhackers.com/store/3d-printer-filament/ninjaflex-water-semi-transparent-tpe-3d-printing-filament-1.75mm

[21] B. Khatri, K. Lappe, D. Noetzel, K. Pursche, T. Hanemann, A 3D-printable polymer-metal soft-magnetic functional composite—development and characterization, Materials 11 (2) (2018) 189, doi:10.3390/ma11020189.

[22] E.M. Palmero, D. Casaleiz, J. de Vicente, J. Hernández-Vicen, S. López-Vidal, E. Ramiro, A. Bollero, Composites based on metallic particles and tuned filling factor for 3D-printing by fused deposition modeling, Composites, Part A 124 (2019) 105497, doi:10.1016/j.compositesa.2019.105497.

[23] W.D. Callister Jr., D.G. Rethwisch, in: Materials Science and Engineering: An Introduction, 8th ed., Wiley, 2009, pp. 630–631.

[24] L.M. Bollig, M.V. Patton, G.S. Mowry, B.B. Nelson-Cheeseman, Effects of 3-D printed structural characteristics on magnetic properties, IEEE Trans. Magn. 53 (11) (2017) 1–6, doi:10.1109/tmag.2017.2698034.

[25] C. Huber, S. Cano, I. Teliban, S. Schuschnigg, M. Groenefeld, D. Suess, Polymer-bonded anisotropic srfe12o19filaments for fused filament fabrication, J. Appl. Phys. 127 (6) (2020) 063904, doi:10.1063/1.5139493.

[26] A.K. Bastola, M. Paudel, L. Li, Line-patterned hybrid magnetorheological elastomer developed by 3D printing, J. Intell. Mater. Syst. Struct. 31 (3) (2020) 377–388, doi:10.1177/1045389x19891557.